Bull. Mater. Sci. (2023)46:37
https://doi.org/10.1007/s12034-022-02866-3

Intriguing metal–semiconductor transport properties on Se-substituted β-Zn_4Sb_3 compounds

N KARTHIKEYAN[1,*], B KAVIN KUMAR[2], G SATHISH KUMAR[3] and R AKILAN[4]

[1]Department of Physics, Anna University, Chennai 600025, India
[2]Department of Physics, D. G. Vaishnav College, Chennai 600106, India
[3]Department of Physics, Sri Sai Ram Engineering College, Chennai 600044, India
[4]Faculty of Science, Aksheyaa College of Arts and Science, Chennai 603314, India
*Author for correspondence (karthin10@gmail.com)

MS received 3 June 2022; accepted 4 October 2022

Abstract. Among the numerous thermoelectric compounds, β-Zn_4Sb_3 has gained significant interest as a promising thermoelectric material due to its effective working temperature range and enhanced figure of merit (ZT) values. In this work, the effect of Se doping in β-Zn_4Sb_3 system has been studied. The structure refinement of the prepared $Zn_{3.9}Se_{0.1}Sb_3$ solid solution was carried out using Rietveld refinement analysis, which confirms that the compound crystallizes in hexagonal rhombohedric structure with R-3c space group. Temperature-dependent electrical conductivity (σ) of the sample has been measured in the temperature range of 300–610 K. At room temperature, the electrical conductivity value of the sample was found to be high ($\sim$1919 S m^{-1}) and it tends to decrease upon increasing the temperature up to 514 K and thereafter slightly increases, which indicates the typical metallic to semiconductor transition behaviour of the prepared compound. The positive Hall coefficient (R_H) value reveals that the holes are the dominant charge carriers (p-type) in the prepared sample. The power factor value (σS^2) of the sample increases linearly with increase in temperature up to 610 K. Hence the Se substitution in pristine Zn_4Sb_3 possesses greater effect in inducing superior thermoelectric power factor values. Temperature-dependent total thermal conductivity (κ_{total}) of $Zn_{3.9}Se_{0.1}Sb_3$ sample is measured in the temperature range of 300 to 610 K. At room temperature, the κ_{total} value of the sample was found to be very low ($\sim$1 Wm^{-1} K^{-1}) and it decreases linearly with increasing the temperature. At 610 K, the sample shows merely ultra-low-thermal conductivity value ($\sim$0.6 Wm^{-1} K^{-1}). A peak ZT value of $\sim$0.3 was obtained in $Zn_{3.9}Se_{0.1}Sb_3$ solid solution at 610 K, which was found to be quite competitive with the current thermoelectric materials.

Keywords. Energy; thermoelectrics; high temperature; thermoelectric power factor; figure of merit.

1. Introduction

Thermoelectric materials have gained huge consideration in the present decade due to the ability of direct conversion between thermal and electrical energy [1–3]. Materials possessing figure of merit (ZT) value above 1 are considered to be efficient thermoelectric materials to be utilized in thermoelectric generators [4,5]. Among various materials possessing thermoelectric properties, the β-Zn_4Sb_3 compound is considered to be as a state of the art thermoelectric materials that exhibits exceptional thermoelectric property in the intermediate temperature range (470–680 K) and still efforts are being taken to increase its figure of merit value by the way of effective substitution [6–9]. β-Zn_4Sb_3 compound crystallizes with hexagonal rhombohedral crystal structure with R3c space group and it contains 66 atoms per unit cell. Its high efficiency to exhibit high electrical transport properties like doped semiconductor is its distinctive property [10,11]. On the other hand, Zn_4Sb_3 is known as the economically cheaper thermoelectric material with less toxic components, which roots their prospective commercial applicability [12,13]. The origin of the enhanced thermoelectric property of β-Zn_4Sb_3 compound is quite comparable with the presence of disorder in the Zn substructure, which occurs due to the combination of defects and interstitial sites [14–18]. Particularly these structural peculiarities restrict the heat-carrying phonons to attain ultra-low-thermal conductivity values [19]. The β-Zn_4Sb_3 compound possesses exceptional property such as exhibiting high electrical transport properties like doped semiconductors and low thermal conductivity like glass, the phenomenon is explained by phonon-glass electron concept (PEGC) [20–22]. Recent past numerous attempts have been carried out on doping different elements in the β-Zn_4Sb_3 host compound and few have achieved great enhancement in the ZT values such as Zn_4sb_3 with Bi, Zn_4Sb_3 with Cd Zn_4Sb_3 with Te Zn_4sb_3 with Gd Zn_4sb_3 with Sn [22–26]. But, the original ZT value of Zn_4Sb_3 materials is a

Published online: 27 February 2023

complicated part to predict, as it has been shown in many studies that on increasing the temperature, Zn_4Sb_3 compound decomposes at a temperature below the anticipated stability range by forming ZnSb and the element Zn has retained as a secondary phase [27]. In the present work, an effort has been taken to study the thermoelectric property of Zn_4Sb_3 compound by doping Se in the Zinc site [28]. This approach has been carried out to achieve low-thermal conductivity in the Zn_4Sb_3 compound by adjusting the carrier concentration and the results obtained from the characterization analysis are discussed in detail.

2. Experimental

The $Zn_{3.9}Se_{0.1}Sb_3$ solid solution was prepared using sealed tube solid-state reaction method. High-purity zinc shots (99.999%), antimony shots (99.99%) and selenium powders (99.99%) purchased from Alfa Aesar were used without further purification. Stoichiometric amount of the starting materials was taken in a quartz tube and flame sealed under vacuum pressure, high vacuum of 10^{-6} mbar. The filled tube was then kept in a high temperature furnace and heated to 600 °C for 10 h and held for 36 h in the same temperature and cooled to room temperature by turning off the furnace. After breaking the quartz tube, average sized ingot was obtained. Further the obtained ingot was well ground and cylindrical pellets were made by hot pressing technique at 500°C with 30 MPa pressure for 20 min.

The powder X-ray diffraction data of the $Zn_{3.9}Se_{0.1}Sb_3$ compound was collected using Bruker D2 PHASER X-ray diffractometer (CuKα, λ = 1.5418 Å) in the 2θ range of 10° to 80° with a step size of 0.02 for 2 h. The fundamental electrical parameters such as carrier concentration, Hall voltage, Hall mobility and electrical conductivity of the prepared sample were examined using ECOPIA HMS 300 Hall effect measurement system at room temperature. Square samples of dimension 8.5 mm were used and the silver paste soldering was done over the corners of the samples for better electrical contact. The densified pellets were cut into ∼1.5 mm of thickness, ∼10 mm of diameter disks and ∼9×3.5×1.8 mm (l×h×w) cuboids for thermal and electrical transport measurements, respectively. The electrical resistivity and Seebeck coefficient of the sample were measured using home-made electrical transport property measurement system. The thermal conductivity (κ) of the samples has been derived from the measurement of thermal diffusivity (D), specific heat capacity (C_p) and density of the sample. In the present study, the parameters 'D' and 'C_p' (using standard sample pyroceram) are directly measured using NETZSCH laser flashline apparatus LFA-457 under nitrogen atmosphere. The cylindrical pellets of 8 mm diameter and 1.5 mm thickness are used for the analysis. The density of the sample is determined from dimension of the sample, which is ∼97% of the theoretical density. The Raman spectra of all the compounds are collected using Horiba Jobin-Yvon, HR 800 UV model spectrometer with an excitation source of 488 nm from He-Ne laser system.

3. Results and discussion

3.1 *Structural characterization*

The crystal structure analysis of the prepared $Zn_{3.9}Se_{0.1}Sb_3$ sample was examined using powder X-ray diffraction

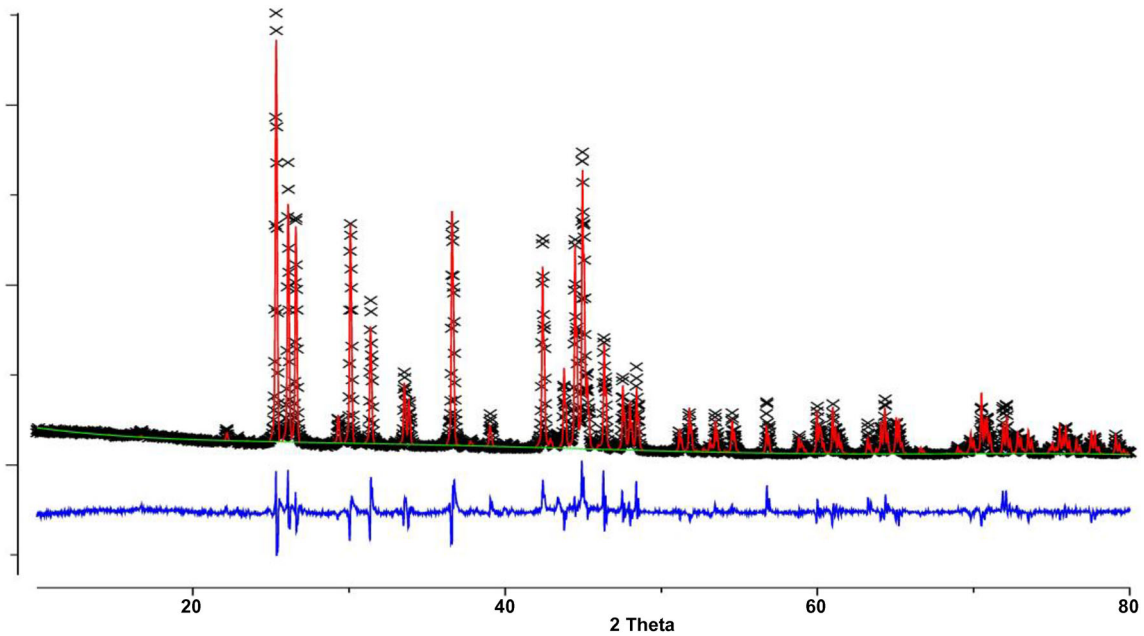

Figure 1. Rietveld refinement plot of $Zn_{3.9}Se_{0.1}Sb_3$. Blue curve: observed pattern, red curve: calculated pattern, grey curve: difference patterns.

Table 1. Crystal data and structure refinement details of $Zn_{3.9}Se_{0.1}Sb_3$ retrieved during Rietveld refinement process.

	$Zn_{3.9}Se_{0.1}Sb_3$
Space group	R-3cH
a	12.26 (7) Å
c	12.45 3) Å
Volume	1620.56 (8) Å^3
R_{wp} (%)	6.1
R_p (%)	8.8
χ^2	3.4

studies. Rietveld refinement of $Zn_{3.9}Se_{0.1}Sb_3$ solid solution has been carried out using GSAS computer suite and the observed Rietveld plot of the solid solutions are shown in figure 1. The powder X-ray diffraction analysis reveals that the sample crystallizes in hexagonal rhombohedral structure with R-3c space group. The Rietveld plot clearly shows the coexistence of Zn peaks with the host Zn_4Sb_3 phase without disturbing the parent crystal structure and such effect was also noticed in recent studies [29].

The structural parameters, *R*-factors (R_p and R_{wp}) and goodness of fit (χ^2) retrieved during Rietveld refinement process is given in table 1.

3.2 *Electrical transport properties*

Temperature-dependent electrical conductivity (σ) of the $Zn_{3.9}Se_{0.1}Sb_3$ sample in the temperature range of 300–610 K is shown in figure 2. At about the room temperature, the electrical conductivity value of the $Zn_{3.9}Se_{0.1}Sb_3$ sample was found to be high ($\sim$1919 S m^{-1}) and it tends to decrease upon increasing the temperature up to 514 K and thereafter the value slightly increases till 600 K. Hence it is found that the sample exhibits metal to semiconductor (insulator) transition. Further from the Hall effect measurement, other electrical parameters such as Hall coefficient (R_H), carrier concentration (n) and Hall mobility (μ) were estimated. The positive Hall coefficient (R_H) value reveals that the holes are the dominant charge carriers (p-type) in the prepared sample. The carrier concentration of the $Zn_{3.9}Se_{0.1}Sb_3$ solid solution was calculated using the formula $n = 1/eR_H$, where e is the charge of electron and it was found to be 5.273×10^{18} cm^{-3}. The Hall mobility of the compound was also calculated using the formula $\mu = \sigma/ne$ and it was found to be 2.30×10^2 cm^2 v^{-1} s^{-1}. Hence, the electrical transport analysis confirms that the substitution of Se in Zn_4Sb_3 compound gradually increases the carrier concentration over the pristine compound.

Temperature-dependent Seebeck coefficient (S) value of the $Zn_{3.9}Se_{0.1}Sb_3$ compound ranging 300–610 K is shown in figure 3. The graph clearly depicts that the Seebeck coefficient value of the sample increases gradually with increasing temperature. At room temperature, the Seebeck coefficient value of the title compound was found to be 100 μV K^{-1} and it increases to the extent of 124 μV K^{-1} till 514 K. On further increasing temperature, it was noticed that the Seebeck coefficient value start decreasing, which describes that the compounds were degenerating semiconductor behaviour and the positive sign of the Seebeck coefficient values indicates that p-type semiconducting nature of the prepared $Zn_{3.9}Se_{0.1}Sb_3$ compound.

Using the measured electrical conductivity (σ) and Seebeck coefficient (S) values, the power factor (σS^2) value of the title compound was determined for the temperature range of 300–610 K and is shown in figure 4. The power factor value of the sample increases linearly with increase in temperature up to 510 K. At the room temperature, the power factor value of the sample was found to be 9×10^6 W mK^{-2} and it abruptly increases to

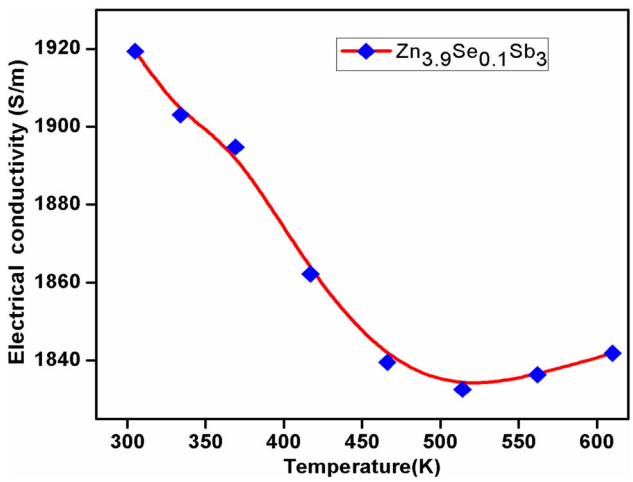

Figure 2. Temperature-dependent electrical conductivity (σ) of the $Zn_{3.9}Se_{0.1}Sb_3$ solid solution.

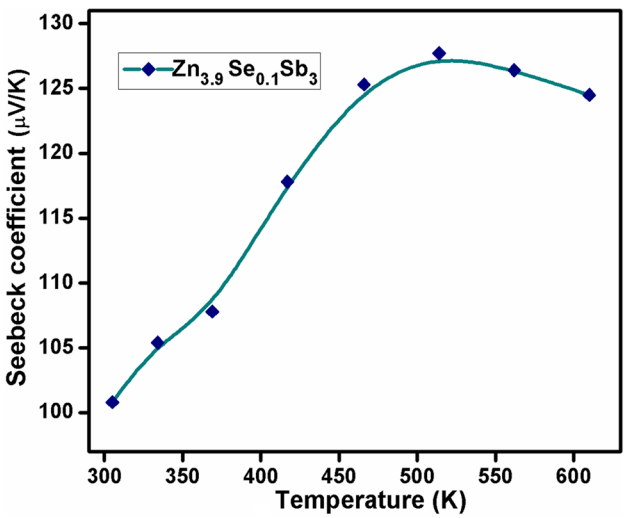

Figure 3. Temperature-dependent Seebeck coefficients (S) of $Zn_{3.9}Se_{0.1}Sb_3$ solid solution.

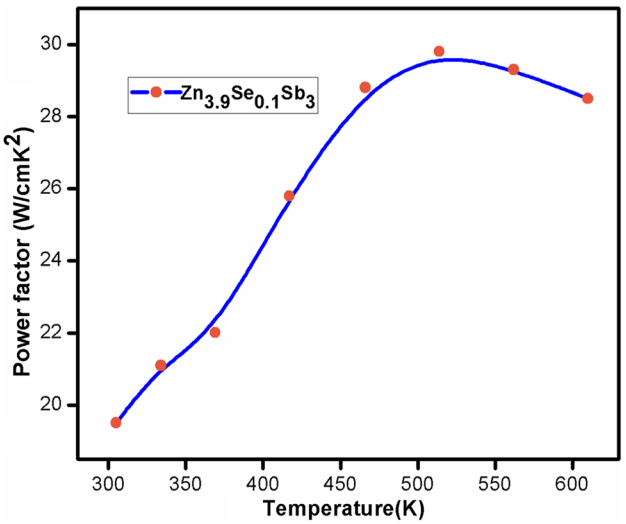

Figure 4. Temperature-dependent power factor ($S2\sigma$) of $Zn_{3.9}Se_{0.1}Sb_3$ solid solution.

24×10^6 W mK^{-2}. Hence, the electrical transport characteristics reveal that the Se-substituted $Zn_{3.9}Se_{0.1}Sb_3$ possesses superior thermoelectric power factor values.

3.3 *Thermal transport properties*

Temperature-dependent total thermal conductivity (κ_{total}) of the $Zn_{3.9}Se_{0.1}Sb_3$ sample in the range of 300 to 610 K is shown in figure 5. The total thermal conductivity (κ_{total}) value of the sample has been determined using the equation $\kappa_{total} = DC_p\rho$, where D is the thermal diffusivity, C_p is specific heat capacity and ρ is density of the sample.

At the room temperature, the κ_{total} value of the sample was found to be very low ($\sim$1 Wm^{-1} K^{-1}) and found with linear decrease with increasing the temperature up to 610 K. At this temperature, the sample shows merely ultra-low-thermal conductivity value ($\sim$0.6 Wm^{-1} K^{-1}). This signifies that the typical lattice contribution in total thermal conductivity, controlled by Umklapp scattering process, dominates the thermal conduction. It is well known that the lattice thermal conductivity (κ_{latt}) can be derived by subtracting the electronic contribution ($\kappa_{elec} = L\sigma T$) from the total thermal conductivity (κ_{total}) based on Wiedemann-Franz law, i.e., $\kappa_{latt} = \kappa_{total} - L\sigma T$, where L is the Lorentz number, σ is the experimental electrical conductivity and T the absolute temperature. The Lorentz number, $L = 2.44\times10^{-8}$ WΩ K^{-2} is a universal constant for non-degenerate materials and it is largely deviated from the value approximately more than 30–40% in the case largely doped semiconductors. Therefore, the value of L with respect to change in temperature can be derived based on the single parabolic band-acoustic phonon scattering (SPS-APS) approximation using the following relation [30]:

$$L = 1.5 + \exp\left[-\frac{|S|}{116}\right] \quad (1)$$

The calculated Lorentz number (L) based on the above equation (1) in the temperature range of 300 to 610 K is depicted in figure 6, which shows notable variation in the L value.

Based on the above considerations, the lattice thermal conductivity (κ_{latt}) of the $Zn_{3.9}Se_{0.1}Sb_3$ was calculated for the temperature range 300 to 610 K. From figure 7, it was inferred that the κ_{latt} values of the sample decreases largely with increasing temperature range.

The κ_{latt} value of the sample is relatively low particularly at higher temperatures, where the high frequency phonons are largely scattered due to phonon−phonon processes at higher temperatures.

3.4 *Debye–Callaway–Klemens model*

The disorder parameters such as imperfection parameter (Γ), mass fluctuation parameter (Γ_m) and strain fluctuation

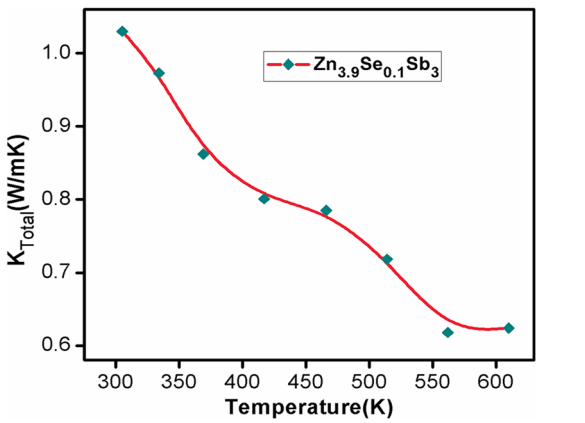

Figure 5. Temperature-dependent total thermal conductivity (κ_{total}) of $Zn_{3.9}Se_{0.1}Sb_3$ solid solution.

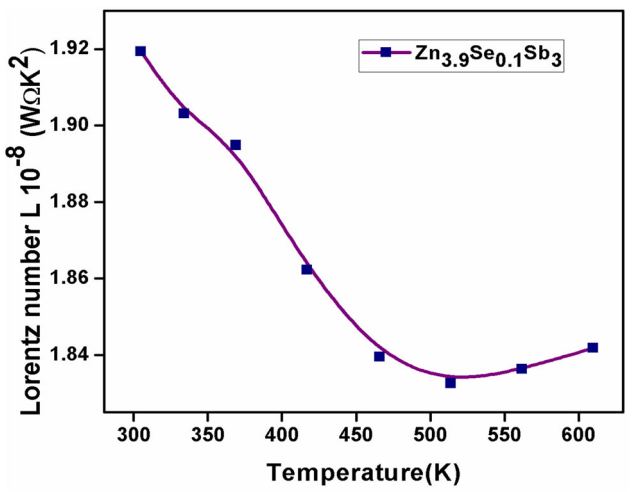

Figure 6. Temperature-dependent Lorentz number of $Zn_{3.9}Se_{0.1}Sb_3$ solid solution.

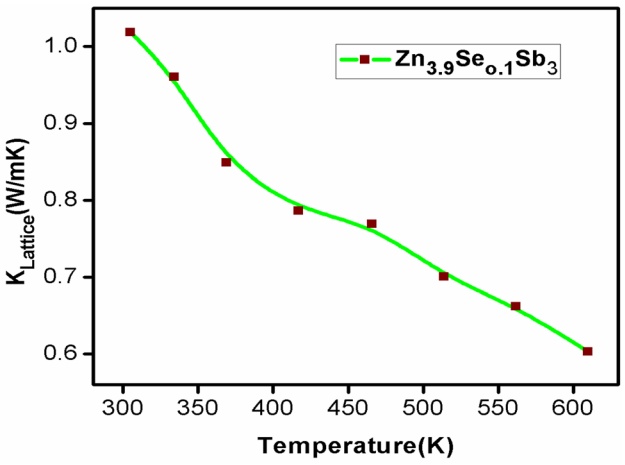

Figure 7. Temperature-dependent lattice thermal conductivity (κ_{latt}) of the $Zn_{3.9}Se_{0.1}Sb_3$ solid solution.

parameter (Γ_s), i.e., $\Gamma = \Gamma_m + \Gamma_s$ has been estimated by Debye-Callaway-Klemens model. It is a theoretical model to examine point defect in the reduction of κ_{latt} due to mass and strain imperfections in doped semiconductor alloys [31,32]. In the present work, the disorder parameters Γ, Γ_m and Γ_s were determined and the values are given in table 2.

3.5 *Raman spectral analysis*

The effect of incorporation of Se atoms into the host lattice of Zn_4Sb_3 compound has been analysed by Raman spectral analysis. Due to displacement of atoms on doping/substitution of foreign atoms, lattice distortion has been induced on specific site occupancy of metal ions and to be analysed by Raman spectroscopic technique. The observed Raman spectra of $Zn_{3.9}Se_{0.1}Sb_3$ compound with excitation source of wavelength 532 nm is shown in figure 8. The observed Raman signals were fitted with Lorentzian line shape to analyse the polarization dependence and it is shown in figure 9. The sharp and distinguished peaks of Raman signals confirm the higher relative density of the compound [33].

From figure 8, the sharp Raman peak is found to be around 102 cm^{-1} explicit the degenerate E_g band and leads to the displacement of atoms perpendicular to the C3 axis. Further, the peak at 152 cm^{-1} reveals the A_g mode and characterizes the shifting of Sb atoms along the C3 axis. Both the peaks at 102 and 152 cm^{-1} confirm the Raman active modes of rhombohedral Sb atoms. The resonance peak around 169 cm^{-1} exhibits the stretching mode of Sb_2 moieties in ZnSb system. The additional degenerate peaks around 91 and 135 cm^{-1} reveal the effect of incorporation of Se ions in the host matrix of Zn_4Sb_3 system. Hence, the effect of incorporation of Se atoms into the ZnSb system

Table 2. Imperfection scaling parameter (Γ), mass fluctuation imperfection parameter (Γ_m) and strain fluctuation imperfection parameter (Γ_s) of the $Zn_{3.9}Se_{0.1}Sb_3$.

	$Zn_{3.9}Se_{0.1}Sb_3$
Γ	0.0206
Γ_m	0.0009
Γ_s	0.0191

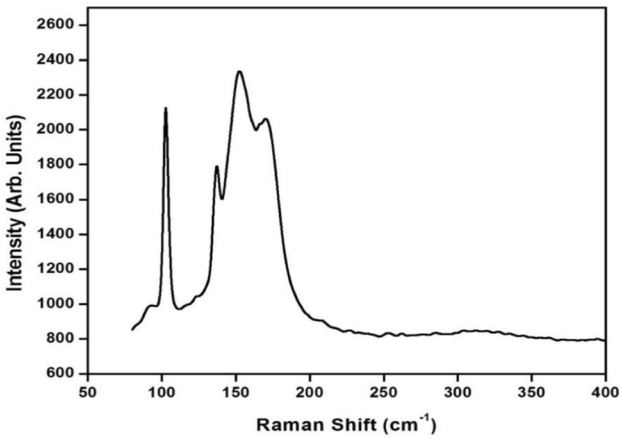

Figure 8. Raman spectra of the $Zn_{3.9}Se_{0.1}Sb_3$ solid solution.

leads to stretching of Sb–Sb bonds and so the Raman active modes arise due to vibrations of filler atoms into the host lattice [34].

Hence, the Raman spectral analysis exhibits the possible substitution/doping of Se atoms into the Zn_4Sb_3 d by inducing distortion in the crystal lattice through stretching of bonds between two nearby cations, which leads to enhancement of phonon–phonon interaction mechanism [35,36].

3.6 *Thermoelectric figure of merit*

Temperature dependence of thermoelectric figure of merit (ZT) for the prepared $Zn_{3.9}Se_{0.1}Sb_3$ solid solution is shown in figure 10. A peak ZT value of $\sim$0.3 is observed in the $Zn_{3.9}Se_{0.1}Sb_3$ solid solution at 610 K, which is one of the notable ZT value in current thermoelectrics but the ZT value was slightly reduced compared to the parent Zn_4Sb_3, as found in the previous literatures [22–25,37,38]. Therefore, the thermoelectric performance can be enhanced by increasing the doping concentration to induce more disorder effect within the material.

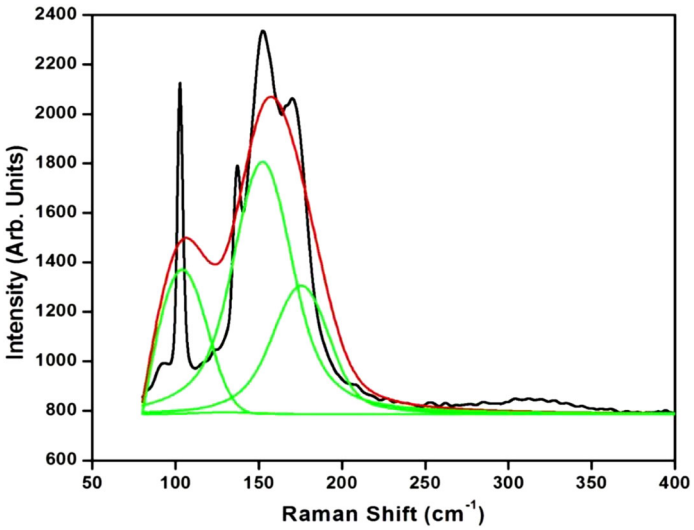

Figure 9. Fitting curves for the Raman signal of $Zn_{3.9}Se_{0.1}Sb_3$ with Lorentzian line shapes.

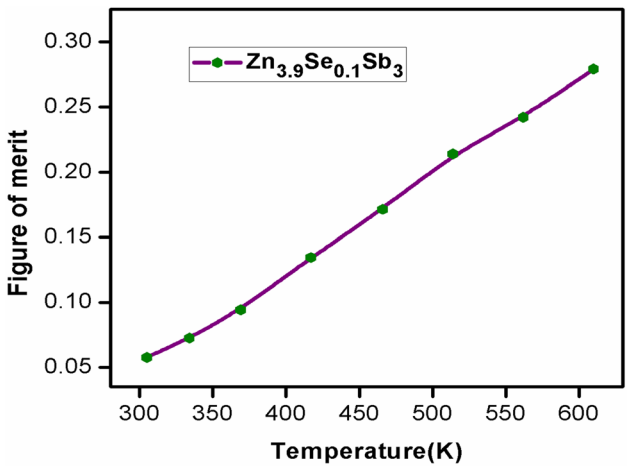

Figure 10. Temperature-dependent dimensionless figure of merit of $Zn_{3.9}Se_{0.1}Sb_3$ solid solution.

4. Conclusion

The influence of Se doping in thermoelectric properties of Zn_4Sb_3 compound has been studied. The phase-pure formation of the prepared solid solution was examined using Rietveld refinement method. The electrical transport studies show that the compounds result in superior power factor values. The Hall effect measurement studies show that the carrier mobility of the solid solution was increased upon the addition of Se. The combination of interstitial disorder of Zn and the increase in disorders due to substitution of impurity (Se) atoms, the solid solution exhibits ultra-low-thermal conductivity values closer to amorphous limit. A peak of ZT value of $\sim$0.3 was obtained with the $Zn_{3.9}Se_{0.1}Sb_3$ solid solution at a temperature of 680 K, which is considered to be one of the notable ZT value in current thermoelectrics. Hence, the thermoelectric performance of solid solution can be further enhanced by increasing the doping concentration of Se into Zn_4Sb_3 to induce more disorder effect.

References

[1] Sootsman J, Chung D Y and Kanatzidis M G 2009 *Angew. Chem. Int. Ed.* **48** 8616
[2] Han M K, Zhou X, Uher C, Kim S J and Kanatzidis M G 2012 *Adv. Energy Mater.* **2** 1218
[3] Snyder G J and Toberer E S 2008 *Nat. Mater.* **7** 105
[4] Bell L E 2008 *Science* **321** 1457
[5] Karthikeyan N, Ramesh Kumar R, Jaiganesh G and Sivakumar K 2018 *Physica B Phys. Condens. Matter* **529** 1
[6] Snyder G J, Christensen M, Nishibori E, Caillat T and Iversen B B 2004 *Nat. Mater.* **3** 458
[7] Caillat T, Fleurial J P and Borshchevsky A 1997 *J. Phys. Chem. Solids* **58** 1119
[8] Bottger P H M, Diplas S, Larsen E F, Prytz O and Finstad T G 2011 *J. Phys: Cond. Matt. Phys.* **23** 265502
[9] Toberer E S, Rauwel P, Gariel S, Tafto J and Snyder G J 2010 *J. Mat. Chem.* **20** 987
[10] Souma T, Nakamoto G and Kurisu M 2002 *J. Alloys Compd.* **340** 2750
[11] Caillat T, Fleurial J P and Borshchevsky A 1997 *J. Phys.: Cond. Matt. Phys.* **58** 1119
[12] Tsutsui M, Zhang L T, Ito K and Yamaguchi M 2004 *Intermetallics* **12** 809
[13] Liu F, Qi X Y and Li D 2007 *J. Phys. D: Appl. Phys.* **40** 4974
[14] Tenga A, Lidin S, Belieres J P, Newman N, Yang W and Haussermann U 2008 *J. A Chem. Soc.* **130** 15564
[15] Nakamoto G, Souma T, Yamaba M and Kurisu M 2004 *J. Alloys Compd.* **377** 59
[16] Record M C, Izard V, Bulanova M and Tedenac J C 2003 *Intermetallics* **11** 1189

[17] Souma T and Ohtaki M 2006 *J. Alloys Compd.* **413** 289
[18] Kuznetsov V L and Rowe D M 2004 *J. Alloys Compd.* **372** 103
[19] Nylen J, Andersson M, Lidin S and Haussermann U 2004 *J. Am. Chem. Soc.* **126** 16306
[20] Slack G A 1995 *CRC Handbook of Thermoelectrics* (Routledge Taylor & Francis Group) 407
[21] Mozharivskyj Y, Janssen Y, Harringa J L, Kracher A, Tsokol A O and Miller G J 2006 *Chem. Mat.* **18** 822
[22] Ren B, Liu M, Li X, Qin X, Li D, Zou T *et al* 2015 *J. Mater. Chem. A* **3** 11768
[23] Nylen J, Lidin S, Andersson M, Liu H, Newman N and Haussermann U 2007 *J. Solid State Chem.* **180** 2603
[24] Lin J, Li X, Qiao X, Whang Z, Carrete J, Ren Y *et al* 2014 *J. Am. Chem. Soc.* **136** 1497
[25] Qin X Y, Liu M, Pan L, Xin H X, Sun J H and Wang Q Q 2011 *J. Appl. Phys.* **109** 033714
[26] Li D and Qin X Y 2011 *Intermetallics* **19** 1651
[27] Pedersen B L, Yin H, Birkedal H, Nygren M and Iverse B B 2010 *Chem. Mater.* **22** 2375
[28] He X, Fu Y, Singh D J and Zhang L 2016 *J. Mater. Chem. C* **4** 11305
[29] Iversen B B 2010 *J. Mater. Chem.* **20** 10778
[30] Beekman M, Morelli D T and Nolas G S 2015 *Nat. Mater.* **14** 1182
[31] Abeles B 1963 *Phys. Rev.* **131** 1906
[32] Karthikeyan N, Ghanta S, Mishra S, Jaiganesh G, Anbarasu V, Jana P P *et al* 2017 *J. Alloys Compd.* **729** 303
[33] Callaway J and Vonbaeyer C 1960 *Phys. Rev.* **120** 1149
[34] Wan C L, Pan W, Xu Q, Qin Y X, Wang J D, Qu Z X *et al* 2006 *Phys. Rev. B Cond. Matter Mater. Phys.* **74** 144109
[35] Karthikeyan N, Ghanta S, Jaiganesh G, Anbarasu V, Jana P P and Sivakumar K 2017 *Phys. Chem. Chem. Phys.* **19** 28116
[36] Karthikeyan N, Jaiganesh G, Anbarasu V, Jana P P and Sivakumar K 2018 *Mater. Today Comm.* **14** 128
[37] Zou T, Qin X, Zhang Y, Li X, Zeng Z, Li D *et al* 2015 *Sci. Rep.* **5** 17803
[38] Wu H-J, Wei P-C, Su H-Y, Wang K-K, Yen W-T, Jen I-L *et al* 2019 *ACS Appl. Energy Mater.* **2** 7564